

Energetic Electron Irradiations of Amorphous and Crystalline Sulphur-Bearing Astrochemical Ices

Duncan V. Mifsud^{1,2,*}, Péter Herczku^{2,*}, Richárd Rácz², K.K. Rahul², Sándor T.S. Kovács², Zoltán Juhász², Béla Sulik², Sándor Biri², Robert W. McCullough³, Zuzana Kaňuchová⁴, Sergio Ioppolo⁵, Perry A. Hailey¹, and Nigel J. Mason^{1,2,*}

1 *Centre for Astrophysics and Planetary Science, School of Physical Sciences, University of Kent, Canterbury CT2 7NH, United Kingdom*

2 *Institute for Nuclear Research (Atomki), Debrecen H-4026, Hungary*

3 *Department of Physics and Astronomy, School of Mathematics and Physics, Queen's University Belfast, Belfast BT7 1NN, United Kingdom*

4 *Astronomical Institute, Slovak Academy of Sciences, Tatranská Lomnica SK-059 60, Slovakia*

5 *School of Electronic Engineering and Computer Science, Queen Mary University of London, London E1 4NS, United Kingdom*

* Correspondence: Duncan V. Mifsud dm618@kent.ac.uk
 Péter Herczku herczku@atomki.hu
 Nigel J. Mason n.j.mason@kent.ac.uk

ORCID Identification Numbers

Duncan V. Mifsud	0000-0002-0379-354X
Péter Herczku	0000-0002-1046-1375
Richard Rácz	0000-0003-2938-7483
K.K. Rahul	0000-0002-5914-7061
Sándor T.S. Kovács	0000-0001-5332-3901
Zoltán Juhász	0000-0003-3612-0437
Béla Sulik	0000-0001-8088-5766
Sándor Biri	0000-0002-2609-9729
Robert W. McCullough	0000-0002-4361-8201
Zuzana Kaňuchová	0000-0001-8845-6202
Sergio Ioppolo	0000-0002-2271-1781
Perry A. Hailey	0000-0002-8121-9674
Nigel J. Mason	0000-0002-4468-8324

Abstract

Laboratory experiments have confirmed that the radiolytic decay rate of astrochemical ice analogues is dependent upon the solid phase of the target ice, with some crystalline molecular ices being more radio-resistant than their amorphous counterparts. The degree of radio-resistance exhibited by crystalline ice phases is dependent upon the nature, strength, and extent of the intermolecular interactions that characterise their solid structure. For example, it has been shown that crystalline CH₃OH decays at a significantly slower rate when irradiated by 2 keV electrons at 20 K than does the amorphous phase due to the stabilising effect imparted by the presence of an extensive array of strong hydrogen bonds. These results have important consequences for the astrochemistry of interstellar ices and outer Solar System bodies, as they imply that the chemical products arising from the irradiation of amorphous ices (which may include prebiotic molecules relevant to biology) should be more abundant than those arising from similar irradiations of crystalline phases. In this present study, we have extended our work on this subject by performing comparative energetic electron irradiations of the amorphous and crystalline phases of the sulphur-bearing molecules H₂S and SO₂ at 20 K. We have found evidence for phase-dependent chemistry in both these species, with the radiation-induced exponential decay of amorphous H₂S being more rapid than that of the crystalline phase, similar to the effect that has been previously observed for CH₃OH. For SO₂, two fluence regimes are apparent: a low-fluence regime in which the crystalline ice exhibits a rapid exponential decay while the amorphous ice possibly resists decay, and a high-fluence regime in which both phases undergo slow exponential-like decays. We have discussed our results in the contexts of interstellar and Solar System ice astrochemistry and the formation of sulphur allotropes and residues in these settings.

Keywords: Astrochemistry; Planetary science; Electron irradiation; Radiation chemistry; Amorphous ice; Crystalline ice; Sulphur

1 Introduction

It has been established for some time now that the laboratory irradiation of astrochemical ice analogues using energetic charged particles (i.e., ions and electrons) or ultraviolet photons may lead to the production of prebiotic molecules relevant to biology, such as amino acids or nucleobases (e.g., Muñoz-Caro *et al.* 2002, Hudson *et al.* 2008, Nuevo *et al.* 2012). Motivated by a desire to further understand the non-equilibrium chemistry leading to the formation of these so-called ‘seeds of life’, many studies have sought to determine and quantify the influence of various physical parameters on the outcome of such reactions. Perhaps the best studied of these is ice temperature, with previous works having demonstrated the key influence of this parameter on the abundance of product molecules formed after irradiation (e.g., Sivaraman *et al.* 2007, Mifsud *et al.* 2022a).

Our recent work has also demonstrated that the solid phase of an irradiated ice plays a crucial role in determining the outcome of astrochemical reactions mediated by ionising radiation. Through a series of comparative electron irradiations, we have demonstrated that the radiolytic decay rate of an astrochemical ice is dependent upon the nature, strength, and extent of the intermolecular interactions that characterise its solid phase (Mifsud *et al.* 2022b, Mifsud *et al.* 2022c). For instance, the decay rate of α -crystalline CH_3OH was found to be significantly less rapid than that of the amorphous phase. This was attributed to the existence of an extensive network of strong hydrogen bonds that exists in the α -crystalline phase. This network requires an additional energy input from the projectile electrons to be overcome, thus leaving less energy overall to drive radiolytic chemistry. Conversely, the amorphous CH_3OH ice is characterised only by localised clusters of hydrogen bonded molecules. Such a structure does not benefit from the same stabilising effect supplied by the network of hydrogen bonds in the α -crystalline phase, particularly as hydrogen bonding in CH_3OH is known to be a cooperative phenomenon in which the presence of one hydrogen bond in the network strengthens successive hydrogen bonds through electrostatic effects (Kleeberg and Luck 1989, Sum and Sandler 2000).

In the case of N_2O ice, the decay rate of the amorphous phase was noted to be only moderately more rapid than that of the crystalline phase (Mifsud *et al.* 2022b). The dominant intermolecular forces of attraction in solid N_2O are expected to be dipole-dipole interactions. Although the orientation of these dipoles in the crystalline phase is anticipated to confer some degree of resistance against radiolytic decay compared to the amorphous phase, this is considerably less than that induced by the hydrogen bonding network in α -crystalline CH_3OH . This therefore explains the more similar radiolytic decay rates of amorphous and crystalline N_2O . Such results carry important implications for the radiation processing of astrochemical ices, as they suggest that the irradiation of amorphous ices is more chemically productive than that of crystalline ones; particularly in the case of those ices which are able to form strong and extensive intermolecular bonds when crystalline. Extending this idea further, it is entirely possible that those astrophysical environments in which space radiation-induced amorphisation processes dominate over thermally-induced crystallisation may be characterised by a more productive radiation chemistry. This idea is not unreasonable, particularly in light of the discovery of several complex organic molecules in pre-stellar cores (e.g., McGuire *et al.* 2020, Burkhardt *et al.* 2021).

In this present study, we have expounded upon our previous work by performing comparative electron irradiations of the crystalline and amorphous phases of pure H₂S and SO₂ astrochemical ice analogues, thus simulating the processing such ices undergo during their interaction with galactic cosmic rays, stellar winds, or magnetospheric plasmas as a result of the production of large quantities of secondary electrons (Mason *et al.* 2014, Boyer *et al.* 2016). Solid H₂S is known to exhibit a number of stable crystalline phases under low temperature and ambient pressure conditions (Fathe *et al.* 2006), but it is the crystalline phase III (hereafter simply referred to as the crystalline H₂S phase) which is of importance under conditions relevant to astrochemistry. This phase is orthorhombic, having eight molecules per unit cell and adopting the *Pbcm* space group. SO₂ may also exist as an orthorhombic crystalline solid under astrochemical conditions, but in this case the *Aba2* space group is adopted and there are only two molecules per unit cell (Schriver-Mazzuoli *et al.* 2003).

Although sulphur is one of the most abundant elements in the cosmos and is of importance in both biochemical and geochemical contexts, much remains unknown regarding its chemistry in interstellar and outer Solar System settings (Mifsud *et al.* 2021a). It is thought, for instance, that H₂S ice processing by galactic cosmic rays or ultraviolet photons accounts for the apparent depletion of sulphur (relative to its total cosmic abundance) in dense interstellar clouds by producing large quantities of atomic sulphur or molecular sulphur chains and rings which are difficult to detect using current observation techniques (Jiménez-Escobar and Muñoz-Caro 2011, Jiménez-Escobar *et al.* 2014). H₂S itself has not yet been definitively detected in interstellar icy grain mantles (Boogert *et al.* 2015). Conversely, SO₂ ice has been detected within both the dense interstellar medium as well as on the surfaces of outer Solar System bodies such as the Galilean moons of Jupiter (Boogert *et al.* 1997, Carlson *et al.* 1999). However, the exact chemical mechanisms leading to its formation in these settings remain widely debated (Mifsud *et al.* 2021a).

The purpose of this study is thus two-fold: (i) to determine whether the phase of irradiated sulphur-bearing molecular ices influences the radiation-induced rate of decay as was previously demonstrated for non-sulphur-bearing ices; and (ii) to contribute further to our (comparatively poor) understanding of the extra-terrestrial chemistry of sulphur. To achieve these goals, the amorphous and crystalline phases of pure H₂S and SO₂ ices were respectively irradiated with 2 and 1.5 keV electrons, and the resultant physico-chemical changes were followed *in situ* using Fourier-transform mid-infrared (FT-IR) transmission absorption spectroscopy.

2 Experimental Methodology

The irradiation experiments were performed using the Ice Chamber for Astrophysics-Astrochemistry (ICA); a custom-built experimental apparatus located at the Institute for Nuclear Research (Atomki) in Debrecen, Hungary. This apparatus (Fig. 1) has been described in detail in previous publications (Herczku *et al.* 2021, Mifsud *et al.* 2021b), and so only a brief description of the most salient details will be provided here. The ICA is a UHV-compatible chamber with a nominal base pressure of a few 10⁻⁹ mbar which is achieved by the combined action of a dry rough vacuum pump and a turbomolecular pump. Within the centre of the chamber is a gold-coated oxygen-free copper sample holder which supports up to four ZnSe deposition substrates, onto which astrochemical ice analogues may be prepared. The

temperature of the sample holder and the substrates may be cooled to 20 K using a closed-cycle helium cryostat, although an operational temperature range of 20-300 K is available.

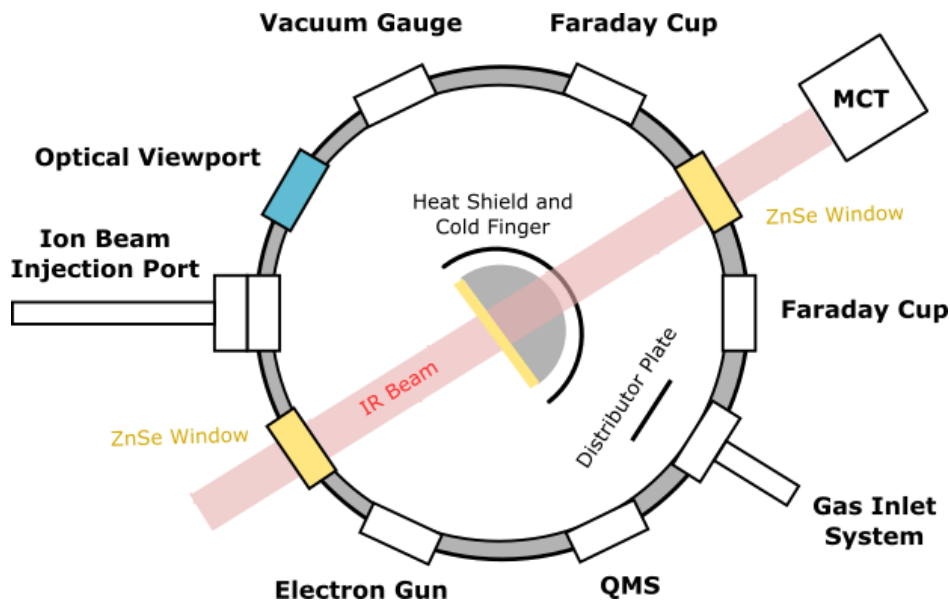


Fig. 1: Top-view schematic diagram of the ICA set-up. Note that electron irradiations are carried out such that projectile electrons impact the target ices at 36° to the normal. Figure reproduced from Mifsud *et al.* (2021b) with the kind permission of the European Physical Journal (EPJ).

The preparation of H_2S and SO_2 astrochemical ice analogue phases was achieved *via* background deposition by allowing the relevant gas into a pre-mixing line before dosing it into the main chamber at a pressure of a few 10^{-6} mbar. Amorphous ice phases were prepared by deposition at 20 K, while crystalline H_2S and SO_2 ices were prepared by deposition at 60 and 90 K, respectively, before being cooled to 20 K. Once deposited, FT-IR spectra (spectral range = $4000\text{-}650\text{ cm}^{-1}$; spectral resolution = 1 cm^{-1}) of the ices were acquired, from which quantitative measurements of their molecular column densities N (molecules cm^{-2}) and thicknesses d (μm) could be performed by measuring the peak area P (cm^{-1}) of a characteristic absorption band (Eq. 1):

$$d = 10,000 \times \frac{NZ}{N_A \rho} = 10,000 \times \ln(10) \times \frac{PZ}{A_v N_A \rho} \quad (\text{Eq. 1})$$

where Z is the molar mass (g mol^{-1}) of the molecular ice, N_A is the Avogadro constant (6.02×10^{23} molecules mol^{-1}), ρ is the density of the ice (g cm^{-3}), and A_v is the band strength constant of the characteristic absorption band whose area is being measured (cm molecule^{-1}). Information on the molecular column densities and thicknesses of the ices investigated in this study, as well as the physical parameters used to calculate these values, is given in Tables 1 and 2.

The deposited pure H_2S and SO_2 astrochemical ices were respectively irradiated using 2 and 1.5 keV electron beams (average flux = 4×10^{13} electrons $\text{cm}^{-2}\text{ s}^{-1}$) to a total fluence of about 8.3×10^{16} electrons cm^{-2} , with projectile electrons impacting the target ices at an angle of 36° to the normal. Prior to commencing the irradiations, the beam current, spot size, and profile

homogeneity were determined using the method described by Mifsud *et al.* (2021b). CASINO simulations (Drouin *et al.* 2007) of the trajectory of the electrons as they travelled through the solid ices revealed that the maximum penetration depths of the incident electrons into the H₂S and SO₂ ices were 155 and 70 nm, respectively. FT-IR spectra were collected at several intervals throughout the irradiation process so as to monitor the radiation chemistry occurring. All irradiations were carried out at 20 K so as to preclude any temperature-dependent effects on the mobility of radiolytically derived radicals. Moreover, the irradiation of each ice phase was performed three times so as to ensure good repeatability of the experiment.

Table 1: List of physical parameters and constants used for the quantitative study of the deposited H₂S and SO₂ astrochemical ices.

Physical Parameter	H ₂ S	SO ₂	Reference
Absorption Band Position (cm ⁻¹)	2550	1148	Garozzo <i>et al.</i> (2008) and Hudson and Gerakines (2018)
Amorphous A_v (10 ⁻¹⁷ cm molecule ⁻¹)	1.12	0.22	Garozzo <i>et al.</i> (2008) and Hudson and Gerakines (2018)
Crystalline A_v (10 ⁻¹⁷ cm molecule ⁻¹)	2.90	0.88	Garozzo <i>et al.</i> (2008) and Hudson and Gerakines (2018)
Amorphous $T_{\text{deposition}}$ (K)	20	20	This work
Crystalline $T_{\text{deposition}}$ (K)	60	90	This work
$T_{\text{irradiation}}$ (K)	20	20	This work
Z (g mol ⁻¹)	34	64	This work
Density (g cm ⁻³)	1.22	1.89	Post <i>et al.</i> (1952) and Yarnall and Hudson (2022)
E_{electron} (keV)	2.0	1.5	This work
Maximum Electron Penetration Depth (nm)	155	70	Drouin <i>et al.</i> (2007)

Table 2: List of initial molecular column densities and thicknesses of the H₂S and SO₂ ices investigated in this study.

Ice	Species	Phase	N (10 ¹⁷ molecules cm ⁻²)	d (μm)
1	H ₂ S	Amorphous	7.05	0.326
2	H ₂ S	Amorphous	6.50	0.301
3	H ₂ S	Amorphous	7.67	0.355
<i>Average</i>			<i>7.07</i>	<i>0.327</i>
4	H ₂ S	Crystalline	5.78	0.268
5	H ₂ S	Crystalline	6.35	0.294
6	H ₂ S	Crystalline	7.61	0.352
<i>Average</i>			<i>6.58</i>	<i>0.305</i>
7	SO ₂	Amorphous	3.09	0.174
8	SO ₂	Amorphous	2.49	0.140
9	SO ₂	Amorphous	2.89	0.162
<i>Average</i>			<i>2.82</i>	<i>0.159</i>
10	SO ₂	Crystalline	2.62	0.147
11	SO ₂	Crystalline	2.19	0.123
12	SO ₂	Crystalline	2.84	0.160
<i>Average</i>			<i>2.55</i>	<i>0.143</i>

3 Results and Discussion

The FT-IR spectra of the pure H₂S and SO₂ ice phases investigated in this study, both before and after irradiation by electrons at different fluences, are depicted in Fig. 2. In the amorphous

phase, H₂S presents a very broad absorption band which peaks at 2550 cm⁻¹ attributable to both the symmetric (ν_1) and asymmetric (ν_3) stretching modes. In the crystalline phase, this band is better resolved and the individual contributors may be observed. The asymmetric stretching mode is observed to peak at 2546 cm⁻¹, while the symmetric stretching mode is split into two components peaking at 2534 and 2522 cm⁻¹. Fathe *et al.* (2006) also observed this splitting and attributed it to the existence of two unique sulphur atoms and three unique S–H bonds in the unit cell.

The amorphous phase of solid SO₂ presents two distinct albeit broad absorption asymmetric and symmetric stretching mode bands which respectively peak at 1320 and 1148 cm⁻¹. In the crystalline phase, these bands are observed to be better resolved, with three and two individual structures being observed in the asymmetric and symmetric stretching mode bands, respectively. These structures have been attributed to the various isotopologues of SO₂ (Schrivier-Mazzuoli *et al.* 2003): the bands peaking at 1323, 1309, 1303, and the shoulder band at 1301 cm⁻¹ are ascribed to the transverse B₁(TO) and B₂(TO) modes of ³²S¹⁶O₂, and to ³⁴S¹⁶O₂ and ³²S¹⁶O¹⁸O; while those peaking at 1143 and 1140 cm⁻¹ are respectively attributed to the transverse A₁(TO) mode of ³²S¹⁶O₂ and to ³⁴S¹⁶O₂. It is interesting to note that the naturally low abundances of ³⁴S and ¹⁸O do not result in weaker band intensities for the SO₂ isotopologues containing these isotopes due to intermolecular coupling between these isotopologues in the condensed phase (Brooker and Chen 1991, Schrivier-Mazzuoli *et al.* 2003).

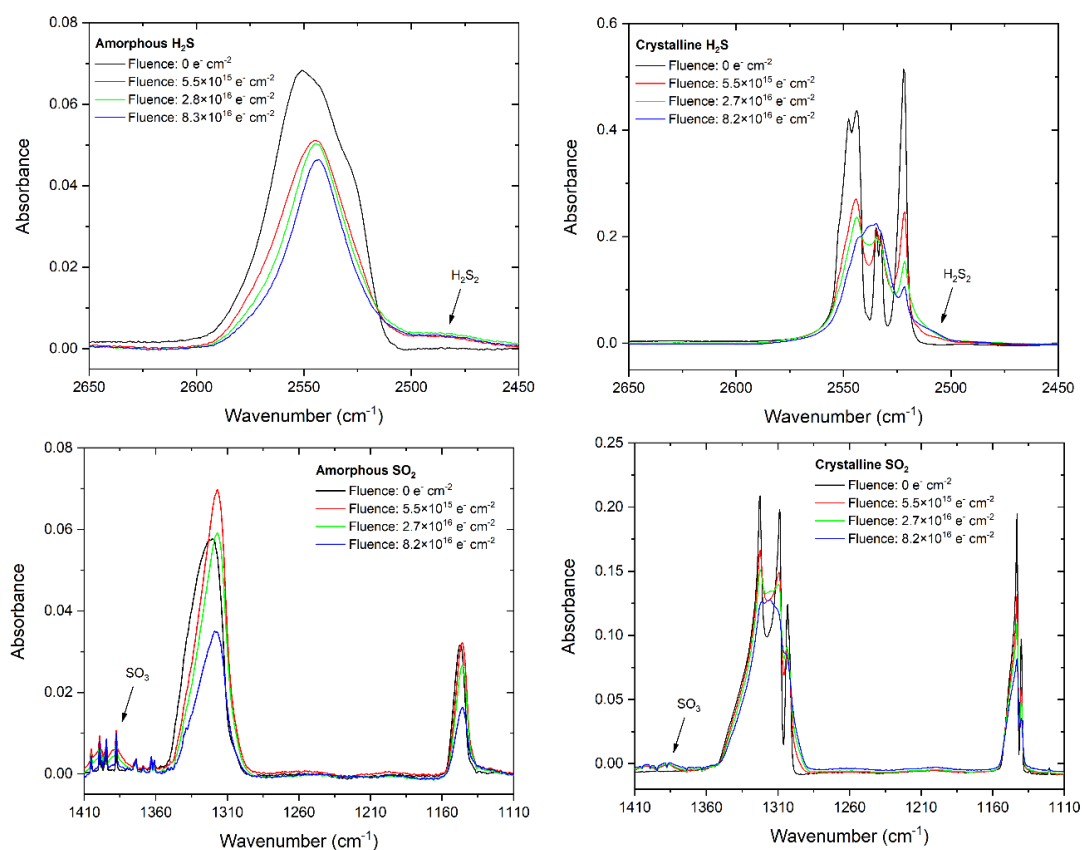


Fig. 2: FT-IR spectra of the amorphous and crystalline phases of H₂S and SO₂ ices at several points during their irradiation by energetic electrons at 20 K. Note that the fine structures coincident with the SO₃ absorption band in the spectrum of the electron irradiated amorphous SO₂ ice are caused by instabilities in the purge of the detector. Moreover, the initial increase in the intensity of the amorphous SO₂ asymmetric stretching mode is likely caused by the radiation-induced compaction of the porous ice.

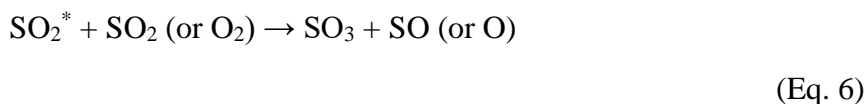
The onset of electron irradiation brings about noticeable changes in the appearances of the spectra of the pristine ices. Perhaps the most prominent of these is the significant broadening of the crystalline ice absorption bands, which also lose their resolved individual structures. This is due to radiation-induced amorphisation, which has been well documented in several ice species irradiated by ions, electrons, and ultraviolet photons; including H₂O, CH₃OH, N₂O, and NH₃ (e.g., Kouchi and Kuroda 1990, Moore *et al.* 2007a, Famá *et al.* 2010, Mifsud *et al.* 2022b, Mifsud *et al.* 2022c). It is interesting to note that, even at the end of the irradiation process once a fluence of $>8 \times 10^{16}$ electrons cm⁻² has been delivered to the crystalline ices, the appearances of their absorption bands are still not identical to those of the deposited amorphous ices. Indeed, small signs of crystallinity (e.g., the presence of shoulder bands or shifted band peak positions) are still observable in the crystalline ices at the end of irradiation. As such, these irradiated ices are likely largely amorphous but with some small degree of remnant structural order.

The irradiation of molecular ices is known to initiate a rich chemistry leading to the formation of new species. Previous studies have established that irradiated H₂S ices efficiently yield H₂S₂ as well as higher order polysulphanes (H₂S_{*x*}, where *x* > 2) in addition to allotropic forms of elemental sulphur (Shingledecker *et al.* 2020, Cazaux *et al.* 2022). In our experiments, we have observed the formation of H₂S₂ through the development of its vibrational stretching modes which appear as a broad shoulder band on the lower wavenumber end of the analogous H₂S absorption bands at about 2500 cm⁻¹ (Fig. 2; Moore *et al.* 2007b). The chemistry leading to the formation of H₂S₂ (as well as higher order polysulphanes) is thought to be largely mediated by HS radicals formed *via* the dissociation of the parent H₂S molecules:



It should be noted that HS radicals produced as a result of the radiolytic dissociation of H₂S may pick up an electron to form HS⁻ ions. These HS⁻ ions may possibly participate in chemistry leading to the formation of other HS radicals *via* proton abstraction reactions with H₂S, after which the resultant HS⁻ ion may undergo electron auto-detachment to yield HS. A similar process has recently been demonstrated to occur in H₂O ice with respect to radiolytically derived OH radicals and OH⁻ ions (Kitajima *et al.* 2021).

The irradiation of the SO₂ ice phases was also observed to lead to the formation of new molecules; in particular SO₃ which was observed through its asymmetric stretching absorption band at 1388 cm⁻¹ (Guldan *et al.* 1995). SO₃ formation in irradiated SO₂ ices has been studied extensively and is believed to be the result of the dissociation of the latter species to yield free oxygen atoms which may then bond with other SO₂ molecules (Moore *et al.* 2007b). It should be noted, however, that earlier studies by Pilling and Bergantini (2015) and de Souza Bonfim *et al.* (2017) have demonstrated that electronically excited SO₂ may also abstract oxygen atoms from either an adjacent SO₂ molecule or from a O₂ molecule; the latter having likely been formed as a result of the double ionisation of the SO₂ parent molecule followed by electron neutralisation as described recently by Wallner *et al.* (2022):



Differences in the parent molecule decay trends and in the abundance of molecular products observed after irradiation were noted between the studied amorphous and crystalline ice phases. Considering first the decay trends of the amorphous and crystalline H₂S ices: it was noted that the rate of decay of the crystalline phase was significantly slower than that of the amorphous phase (Fig. 3). A similar trend was observed during the comparative electron irradiations of the amorphous and crystalline phases of CH₃OH, N₂O, and H₂O ices (Mifsud *et al.* 2022b, Mifsud *et al.* 2022c). This was attributed to the additional energy input required to disrupt the extensive intermolecular forces of attraction that characterise the crystalline solid before radiolytic chemistry as a result of molecular dissociation may proceed. In CH₃OH, the α -crystalline phase contains extensive arrays of cooperative and strong hydrogen bonds which stabilise the ice considerably against radiolytic decay compared to the amorphous solid, which is only characterised by localised hydrogen bonds (Kleeberg and Luck 1989, Sum and Sandler 2000, Mifsud *et al.* 2022b).

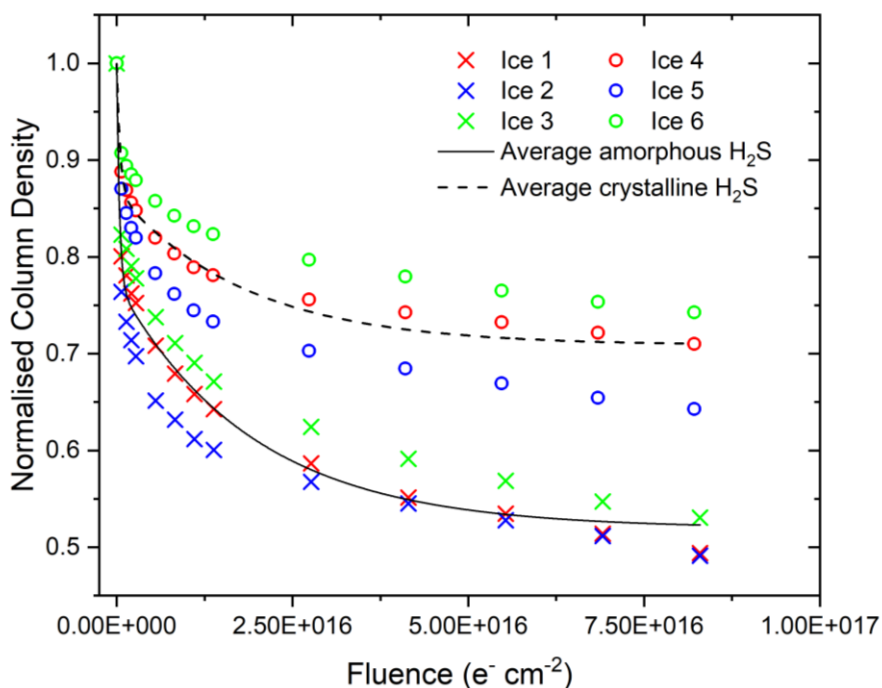


Fig. 3: Decay of amorphous and crystalline H₂S column densities normalised to the initially deposited column density during irradiation using 2 keV electrons. Note that the average decay trends are fitted by two exponential decay functions joined at a fluence of 1.4×10^{15} electrons cm^{-2} .

H₂S is also capable of forming hydrogen bonds between adjacent molecules (Das *et al.* 2018), although these are significantly weaker than those in alcohols: the hydrogen bond strengths in

pure CH₃OH and H₂S are 6.3 and 1.0 kcal mol⁻¹, respectively (Pellegrini *et al.* 1973, Bhattacharjee *et al.* 2013). Despite this weaker nature of the hydrogen bond in H₂S, it still displays a relative stability of the crystalline phase to radiation-induced decay (compared to the amorphous phase) that is qualitatively similar to that of CH₃OH. As such, it is likely that another factor should be invoked to account for the relative radio-resistance of the crystalline phases of these ices; that of lattice energies. The energetic advantage induced by the ordering of the molecular components of the solid ice must also be overcome and thus a proportion of the incident electrons' kinetic energy must be expended upon overcoming both the lattice energy as well as the more extensive hydrogen bonding network in the crystalline phase, leaving less energy to induce the molecular dissociation that drives radiolytic chemistry.

Such an interpretation is wholly consistent with our previously reported results on the comparative electron irradiations of amorphous and crystalline N₂O, which demonstrated only a moderately more rapid decay rate of the former compared to the latter (Mifsud *et al.* 2022b). In that case, a fraction of the kinetic energy of the incident electrons must be used to overcome both the increased ordering of the molecular dipoles as well as the crystal lattice energy. We also note that A_v differs by a factor-of-two-and-a-half between the amorphous and crystalline H₂S phases, with that of the latter being greater. This is not insignificant, and the rapid amorphisation of the crystalline phase as a result of its irradiation may mean that column density measurements of this phase may be somewhat underestimated and, as such, the radio-resistance of the crystalline phase may be even greater than that depicted in Fig. 3, although this is difficult to quantify.

The radiation-induced decay trends of amorphous and crystalline SO₂ (Fig. 4), however, are significantly different to those of H₂S and the previously studied ices. The decay trend of the crystalline SO₂ ice initially exhibits the anticipated profile of a rapid exponential decay. However, once a fluence of about 1.4×10^{16} electrons cm⁻² is exceeded, the normalised column density declines significantly more slowly. Perhaps even more surprising is the fact that the amorphous SO₂ normalised column density (with respect to the initial SO₂ column density deposited) does not really vary at low electron fluences, having an average normalised column density of 0.97 after a fluence of 8.2×10^{15} electrons cm⁻² had been delivered. For comparison, by the point this fluence had been delivered to the crystalline SO₂ ice, its average normalised column density had decreased to 0.83. However, similarly to the case of the crystalline SO₂ ice, once a fluence of about 1.4×10^{16} electrons cm⁻² had been delivered, the normalised column density was observed to undergo a slow exponential-like decay. Interestingly, beyond a delivered fluence of 1.4×10^{16} electrons cm⁻², the rate of decay of the amorphous SO₂ is greater than that of the crystalline SO₂, and indeed the average decay trends cross one another at a fluence of about 5.3×10^{16} electrons cm⁻².

Providing an exact reason for the observed amorphous SO₂ decay trends is a challenging task. Measurements of the photo-desorption of SO₂ molecules from an amorphous ice induced by soft x-rays allowed de Souza Bonfim *et al.* (2017) to suggest that, at low fluences, the recombination of fragments produced by the dissociation of SO₂ to yield electronically excited SO₂ may be a favourable process, thus largely precluding net SO₂ dissociation within the ice. It is also possible that the irradiation of the amorphous SO₂ ice results in its compaction, which may cause an increase in A_v of the measured band (Fig. 2). Similar results were recently shown for ion irradiated amorphous CO ice, for which A_v very rapidly increased by about 5% of its

nominal value as a result of the compaction of the ice (Ivlev *et al.* 2022). It is not possible to discount either of these possible explanations based on the available evidence.

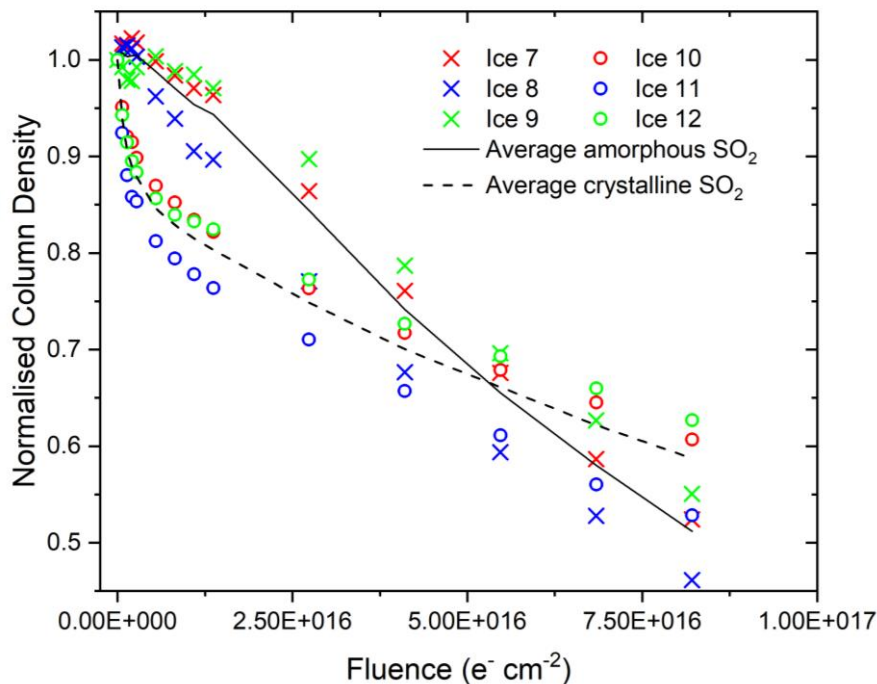


Fig. 4: Decay of amorphous and crystalline SO₂ column densities normalised to the initially deposited column density during irradiation using 1.5 keV electrons. Note that the average decay trends are not fits and are plotted solely to guide the eye.

As a final analytical consideration, we have attempted to establish the sulphur budget of the electron irradiation processes presented in this study. The possible chemical transformations of H₂S and SO₂ to infrared inactive atomic or allotropic forms of sulphur have already been referred to (Shingledecker *et al.* 2020, Cazaux *et al.* 2022), and so it is useful to quantify how much of the initially deposited H₂S or SO₂ ice ends up in such a form as a result of its irradiation. As depicted in Fig. 2, the only major infrared active products of H₂S and SO₂ irradiation were H₂S₂ and SO₃, respectively. We have quantified the column densities of these product molecules throughout the irradiation processes by measuring the peak areas of their primary absorption bands and making use of Eq. 1 (Fig. 5). We note that we have taken A_v for the H₂S₂ absorption band at about 2500 cm⁻¹ to be 2.4×10^{-17} cm molecule⁻¹ (Cazaux *et al.* 2022). To the best of our knowledge, A_v has not yet been defined for the SO₃ absorption band at 1388 cm⁻¹, and so we have followed the example of de Souza Bonfim *et al.* (2017) who assumed that this band strength is equal to that of the SO₂ asymmetric stretching mode which is 1.47×10^{-17} cm molecule⁻¹ (Garozzo *et al.* 2008).

As expected, the yield of H₂S₂ from the irradiated amorphous H₂S ice is greater than that from the irradiated crystalline H₂S ice, commensurate with the increased decay rate of the former compared to the latter. Conversely, the electron irradiation of the crystalline SO₂ ice proved to be more conducive to the formation of SO₃ than did the irradiation of the amorphous phase. This is as expected for the low-fluence regime of the irradiation process (up to a fluence of about 5.3×10^{16} electrons cm⁻²), due to the amorphous SO₂ ice possibly resisting radiolytic decay. However, the greater abundance of SO₃ in the irradiated crystalline ices persists even

beyond this fluence, despite the more rapid decay of amorphous SO_2 after this point. It should be noted, however, that after peaking at a fluence of about 5.5×10^{15} electrons cm^{-2} , the SO_3 column density within the irradiated amorphous SO_2 ice also declines slightly (Fig. 5). The concomitant loss of SO_2 and SO_3 from the ice during its irradiation suggests that sulphur is either being converted into a form which is not infrared active (e.g., atomic or allotropic sulphur) or is being desorbed or sputtered from the bulk ice. In either case, however, there is a fraction of the initially deposited sulphur that remains unobserved in the ice.

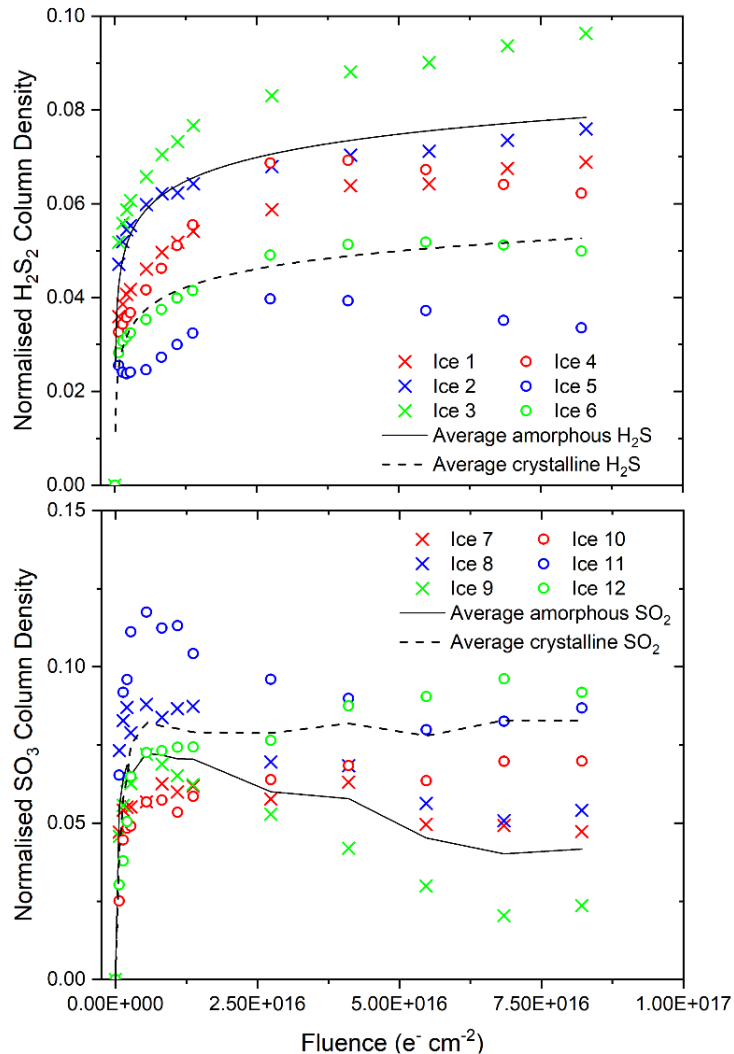


Fig. 5: *Above:* Column density of H_2S_2 from amorphous and crystalline H_2S ices irradiated using 2 keV electrons at 20 K. *Below:* Column density of SO_3 from amorphous and crystalline SO_2 ices irradiated using 1.5 keV electrons at 20 K. Column densities have been normalised to the initially deposited column density of the parent molecular ice. Note that in the case of H_2S_2 the average trends are fitted by logarithmic functions while in the case of SO_3 the average trends are not fits and are plotted solely to guide the eye.

The sulphur budgets of each of the irradiated ices considered in this study are shown in Fig. 6. It is possible to note that a loss of sulphur is observed upon supplying an initial electron fluence of 6.9×10^{14} electrons cm^{-2} in all of the ices apart from the amorphous SO_2 ice, and that the quantity of unobserved sulphur as a fraction of that initially deposited continually grows during irradiation. In the case of the amorphous SO_2 ice, unaccounted for sulphur is only registered

after a fluence of 2.7×10^{16} electrons cm^{-2} has been supplied, possibly due to the resistance of SO_2 to radiolytic dissociation as discussed earlier (de Souza Bonfim *et al.* 2017).

Although it is possible that electron irradiation resulted in the sputtering or desorption of the parent ice species, we consider this process to have likely been a relatively minor one. Previous work has shown, for example, that the reactive desorption of H_2S upon its formation as a result of the hydrogenation of HS on the surface of an interstellar ice analogue has a probability of 3% per hydrogenation event (Oba *et al.* 2018, Oba *et al.* 2019, Furuya *et al.* 2022), which is small from the perspective of an experimental study. Thus, if the electron-induced sputtering or desorption of sulphur-bearing molecules from the bulk ice is assumed to be negligible, then the fractions of unobserved sulphur shown in Fig. 6 represent the sulphur present in an infrared inactive form, such as atomic sulphur or, more likely, residues composed of sulphur allotropes (Gomis and Strazzulla 2008). Our data therefore suggest an important point with regards to the production of such residues from pure H_2S and SO_2 ices: it is apparent that the irradiation of amorphous ices results in a greater abundance of sulphur residues than does the irradiation of crystalline ices. It should be noted, however, that the conversion of observable molecular sulphur to unobservable residues is very efficient in each of the considered ices, with amorphous H_2S , crystalline H_2S , amorphous SO_2 , and crystalline SO_2 ices respectively showing 41%, 25%, 44%, and 32% conversion of the initially deposited sulphur to residues at the end of irradiation (Fig. 6).

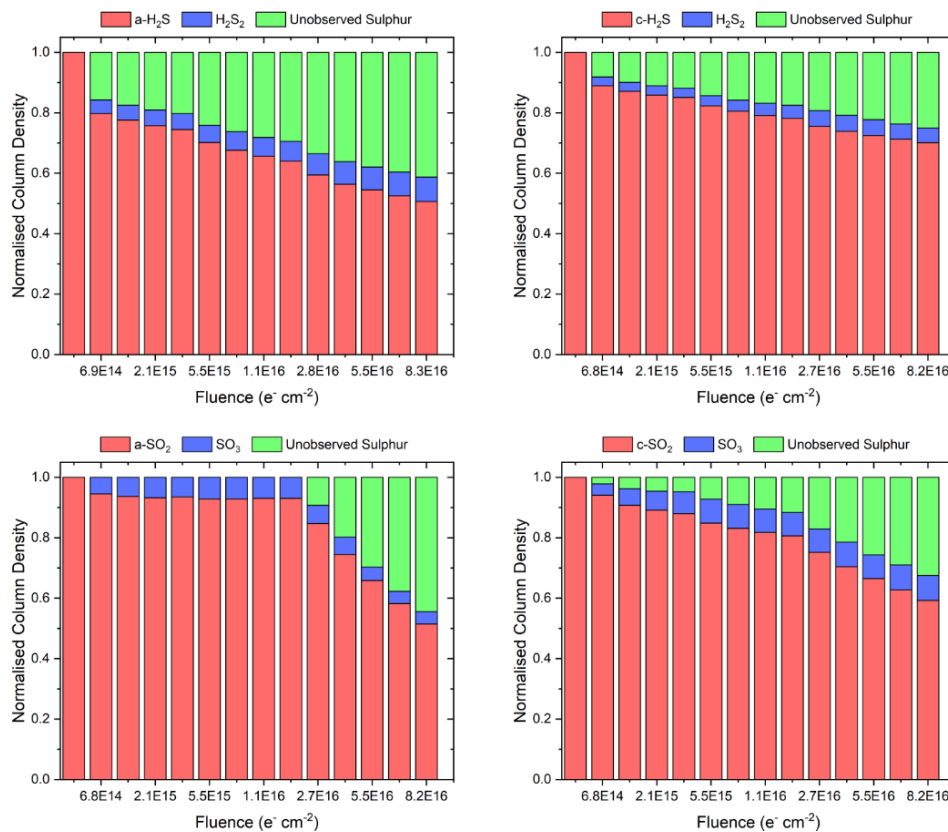


Fig. 6: Sulphur budgets of the electron irradiated amorphous and crystalline H_2S and SO_2 ices considered in this study. Uncertainties in the normalised abundance of the parent and primary product molecules are estimated to be within 3%. The quantity of unobserved sulphur represents an upper bound for the abundance of atomic or allotropic sulphur formed as a result of irradiation, since it is not known how many (if any) sulphur-containing species were sputtered or desorbed from the bulk ice. Note that the notations “a-” and “c-” used in the caption indicate whether the irradiated ice is amorphous or crystalline.

4 Implications for Interstellar and Solar System Chemistry

The results of this present study are directly applicable to the astrophysical chemistry of sulphur. In dense molecular clouds in the interstellar medium, there is a known paucity of observed sulphur relative to its expected cosmic abundance (Tieftrunk *et al.* 1994, Ruffle *et al.* 1999). Recent studies have suggested that this depletion may be mediated by the Coulomb-enhanced freeze-out of sulphur cations onto negatively charged dust grains, whereupon they polymerise to yield sulphur-bearing residues and chains (Cazaux *et al.* 2022). Modelling efforts have suggested different explanations as to the major forms of sulphur in interstellar space: Vidal *et al.* (2017) suggested that, depending upon the age of the dense cloud, the majority of the sulphur exists either as unobservable atoms in the gas phase or as H₂S within icy grain mantles. Navarro-Almaida *et al.* (2020) also suggested the dominance of gas-phase sulphur atoms, whilst Laas and Caselli (2019) concluded that the majority of sulphur is found as organosulphur molecules within the icy grain mantles. Shingledecker *et al.* (2020) proposed that the major sulphur-bearing species in the condensed phase were sulphur allotropes along with SO₂ and OCS.

Nonetheless, it is expected that H₂S will be present within icy grain mantles as a result of the hydrogenation of adsorbed sulphur atoms. Furthermore, SO₂ is suspected to be present in such ices on the basis of its tentative detection (Boogert *et al.* 1997). Our results demonstrate that the irradiation of these ices by galactic cosmic rays (for which we have used an energetic electron beam as a simulant) could further contribute to the presence of sulphur residues, chains, and atoms in the dense interstellar medium and, by extension, could also account for a portion of the depleted sulphur in such regions. Moreover, such processes are likely to be more efficient when the dense cloud is either fairly young (i.e., it is still in its pre-stellar stage) or in those regions of the cloud which are not in proximity to heat sources such as proto-stars since, under such conditions, the interstellar icy grain mantles would not undergo crystallisation or thermal segregation of their molecular constituents and would thus remain amorphous.

Our results are also applicable to outer Solar System chemistry, particularly in the cases of the Galilean moons of Jupiter and of comets. SO₂ is the dominant molecular component of the surface ices and exosphere of the innermost of the Galilean moons; Io (Douté *et al.* 2001), and has also been detected as a component of the icy surfaces of Europa, Ganymede, and Callisto (Noll *et al.* 1995, Noll *et al.* 1997, Domingue *et al.* 1998). Surface temperatures on Io undergo quotidian cycles between 90-130 K, thus allowing for cycles of sublimation and condensation of the surface SO₂ frosts to be maintained (Bagenal and Dols 2020). During the Ionian day, warmer temperatures cause the sublimation of much of the surface SO₂ ice, resulting in the formation of a tenuous exosphere. At night, however, lower temperatures drive the collapse of much of the exosphere and re-condensation of the SO₂ to surface ices.

Given that Io orbits within the giant Jovian magnetosphere, its surface is continually exposed to ionising radiation in the form of energetic ions and electrons. The flux of 0.1-52 keV electrons at the surface of Io was given by Frank and Paterson (1999) to be 3.1×10^8 electrons cm⁻² s⁻¹, meaning the fluence delivered in our experiments would be delivered to the Ionian surface within 8.5 years. The temperature conditions at the surface of Io would lead one to assume that SO₂ ice is naturally found in the crystalline phase, and that, therefore, the radiation-induced formation of SO₃ should be reasonably efficient (Fig. 5). However, our results also demonstrate that the prolonged irradiation of crystalline SO₂ ice at 20 K results in its

amorphisation, reducing the comparative yield of SO_3 in favour of refractory residues of allotropic sulphur (Fig. 6). Such residues may contribute to the distinct colouration of Io (Carlson *et al.* 2007). It should be noted, however, that the extrapolation of radiation-induced amorphisation results acquired at low temperatures to higher ones may not be appropriate. For instance, although the amorphisation of crystalline H_2O is known to occur efficiently as a result of its irradiation at 20 K, this process has never been reported at temperatures >70 K (Mifsud *et al.* 2022c). The efficiency of the radiation-induced crystalline SO_2 ice amorphisation process at various temperatures (including those relevant to the surface of Io) should therefore be tested in future experiments.

Finally, we note that our results are also applicable to the chemistry occurring within the icy nuclei of comets. The recent ESA *Rosetta* mission to comet 67P/Churyumov-Gerasimenko revealed the presence of a number of sulphur-bearing molecules within its icy nucleus, including H_2S , SO_2 , SO , OCS , CS_2 , and S_2 (Rubin *et al.* 2020). As the comet approaches perihelion in its orbit around the sun, thermally-induced crystallisation processes begin to out-compete space radiation-induced amorphisation. Correspondingly, the formation of allotropic sulphur residues *via* the irradiation of the H_2S and SO_2 cometary ice components by the solar wind may decrease slightly in line with the results presented in Fig. 6.

5 Conclusions

In this experimental study, we have performed comparative and systematic electron irradiations of the amorphous and crystalline phases of H_2S and SO_2 ices using 2 and 1.5 keV electrons, respectively. We have shown that, in the case of H_2S , the amorphous parent ice decays at a more rapid rate than does the crystalline one, in a manner that is similar to that previously reported for CH_3OH (Mifsud *et al.* 2022b). This has been attributed to the presence of a more structured and extensive hydrogen bonding system in the crystalline phase compared to the amorphous phase, as well as the inherent lattice energy of the former, which require an additional energy input from the projectile electrons to be overcome before radiolytic chemistry may proceed. The formation of H_2S_2 as a product of the electron irradiation of H_2S occurs to a greater extent in the amorphous phase than in the crystalline phase, in part due to the greater abundance of radiolytically generated HS radicals.

The irradiation of the SO_2 ice revealed unexpected results. In the amorphous ice, two regimes are apparent: a low-fluence regime in which the ice is possibly resistant to radiolytic decay (potentially due to the favourable reformation of excited SO_2 after the dissociation of ground-state SO_2) and a high-fluence regime in which a slow exponential-like decay trend is observed. This contrasts greatly with the crystalline ice, for which a rapid exponential decay is first observed in the low-fluence regime followed by a slower decay (which is slower than that of the amorphous phase) in the high-fluence regime. Interestingly, the formation of SO_3 as a result of the irradiation of the crystalline ice was always greater than during the irradiation of the amorphous ice, possibly due to the initial resistance of the amorphous ice to radiolytic decay and its subsequent preferential formation of infrared inactive sulphur allotropes and residues.

We suggest that our results are important not only in the context of further investigating the phase-dependent radiation chemistry of astrochemical ices, which has thus far been overlooked in the literature, but also in further understanding the chemistry of sulphur in extra-terrestrial environments. Our characterisation of this phase-dependent chemistry is directly applicable to

understanding the sulphur chemistry on the surface of Io, as well as in the icy nuclei of comets. Moreover, our calculated sulphur budgets for each of the irradiation processes considered in this study (which reveal the seemingly efficient formation of infrared inactive sulphur allotropes and residues) may aid in further constraining the exact molecular forms of sulphur in interstellar icy grain mantles and cometary ices. Finally, we conclude by noting that our experimental results further demonstrate the importance of incorporating ice phase as a factor when designing more complete ‘systems astrochemistry’ investigations (Mason *et al.* 2021).

Author Contributions

The experiment was designed by Duncan V. Mifsud and Perry A. Hailey and carried out by Duncan V. Mifsud, Péter Herczku, Sándor T.S. Kovács, Zoltán Juhász, and Béla Sulik. Data analysis was performed by Duncan V. Mifsud, who also wrote the manuscript. All authors were responsible for results interpretation and improvements to the manuscript.

Acknowledgements

The authors gratefully acknowledge funding from the Europlanet 2024 RI which has been funded by the European Union Horizon 2020 Research Innovation Programme under grant agreement No. 871149. The main components of the experimental apparatus were purchased using funding obtained from the Royal Society through grants UF130409, RGF/EA/180306, and URF/R/191018. Recent developments of the experimental set-up were supported in part by the Eötvös Loránd Research Network through grants ELKH IF-2/2019 and ELKH IF-5/2020. We also acknowledge support from the National Research, Development, and Innovation Fund of Hungary through grant No. K128621. Duncan V. Mifsud is the grateful recipient of a University of Kent Vice-Chancellor’s Research Scholarship. The research of Zuzana Kaňuchová is supported by the Slovak Grant Agency for Science (grant No. 2/0059/22) and the Slovak Research and Development Agency (contract No. APVV-19-0072). Sergio Ioppolo acknowledges the Royal Society for financial support. The authors would also like to thank Béla Paripás (University of Miskolc, Hungary) for his continued support and assistance.

References

- Bagenal, F., Dols, V. (2020). The Space Environment of Io and Europa. *J. Geophys. Res. Space Phys.* **125**, e2019JA027485. doi: 10.1029/2019JA027485
- Bhattacharjee, A., Matsuda, Y., Fujii, A., Wategaonkar, S. (2013). The Intermolecular S–H···Y (Y = S, O) Hydrogen Bond in the H₂S Dimer and the H₂S–MeOH Complex. *Chem. Phys. Chem.* **14**, 905. doi: 10.1002/cphc.201201012
- Boogert, A.C.A., Schutte, W.A., Helmich, F.P., Tielens, A.G.G.M., Wooden, D.H. (1997). Infrared Observations and Laboratory Simulations of CH₄ and SO₂. *Astron. Astrophys.* **317**, 929. doi: unknown
- Boogert, A.C.A., Gerakines, P.A., Whittet, D.C.B. (2015). Observations of the Icy Universe. *Annu. Rev. Astron. Astrophys.* **53**, 541. doi: 10.1146/annurev-astro-082214-122348
- Boyer, M.C., Rivas, N., Tran, A.A., Verish, C.A., Arumainayagam, C.R. (2016). The Role of Low-Energy Electrons in Astrochemistry. *Surf. Sci.* **652**, 26. doi: 10.1016/j.susc.2016.03.012
- Brooker, M.H., Chen, J. (1991). Assignment of Transverse Optical-Longitudinal Optical Modes in the Vibration Spectrum of Solid Sulphur Dioxide. *Spectrochim. Acta A: Mol. Biomol. Spectrosc.* **47**, 315. doi: 10.1016/0584-8539(91)80109-V
- Burkhardt, A.M., Lee, K.L.K., Changala, P.B., Shingledecker, C.N., Cooke, I.R., Loomis, R.A., Wei, H., Charnley, S.B., Herbst, E., McCarthy, M.C., McGuire, B.A. (2021). Discovery of the Pure Polycyclic Aromatic Hydrocarbon Indene (c-C₉H₈) with GOTHAM Observations of TMC-1. *Astrophys. J. Lett.* **913**, L18. doi: 10.3847/2041-8213/abfd3a

- Carlson, R.W., Johnson, R.E., Anderson, M.S. (1999). Sulfuric Acid on Europa and the Radiolytic Sulfur Cycle. *Science* **286**, 97. doi: 10.1126/science.286.5437.97
- Carlson, R.W., Kargel, J.S., Douté, S., Soderblom, L.A., Dalton, J.B. (2007). Io's Surface Composition. In: Lopes, R.M.C., Spencer, J.R. (Eds.): *Io After Galileo*. Praxis Publishing Company (Chichester, UK).
- Cazaux, S., Carrascosa, H., Muñoz-Caro, G.M., Caselli, P., Fuente, A., Navarro-Almáida, D., Riviére-Marichalar, P. (2022). Photoprocessing of H₂S on Dust Grains: Building S Chains in Translucent Clouds and Comets. *Astron. Astrophys.* **657**, 100. doi: 10.1051/0004-6361/202141861
- Das, A., Mandal, P.K., Lovas, F.J., Medcraft, C., Walker, N.R., Arunan, E. (2018). The H₂S Dimer is Hydrogen-Bonded: Direct Confirmation from Microwave Spectroscopy. *Angew. Chem. Int. Ed.* **57**, 15199. doi: 10.1002/anie.201808162
- de Souza Bonfim, V., Barbosa de Castilho, R., Baptista, L., Pilling, S. (2017). SO₃ Formation from the X-Ray Photolysis of SO₂ Astrophysical Ice Analogues: FTIR Spectroscopy and Thermodynamic Investigations. *Phys. Chem. Chem. Phys.* **19**, 26906. doi: 10.1039/c7cp03679e
- Domingue, D.L., Lane, A.L., Beyer, R.A. (1998). IUE's Detection of Tenuous SO₂ Frost on Ganymede and its Rapid Time Variability. *Geophys. Res. Lett.* **25**, 3117. doi: 10.1029/98GL02386
- Douté, S., Schmitt, B., Lopes-Gautier, R., Carlson, R., Soderblom, L., Shirley, J., the Galileo NIMS Team (2001). Mapping SO₂ Frost on Io by the Modelling of NIMS Hyperspectral Images. *Icarus* **149**, 107. doi: 10.1006/icar.2000.6513
- Drouin, D., Couture, A.R., Joly, D., Tastet, X., Aimez, V., Gauvin, R. (2007). CASINO V2.42 – A Fast and Easy-to-Use Modeling Tool for Scanning Electron Microscopy and Microanalysis Users. *Scanning* **29**, 92. doi: 10.1002/sca.20000
- Famá, M., Loeffler, M.J., Raut, U., Baragiola, R.A. (2010). Radiation-Induced Amorphisation of Crystalline Ice. *Icarus* **207**, 314. doi: 10.1016/j.icarus.2009.11.001
- Fathe, K., Holt, J.S., Oxley, S.P., Pursell, C.J. (2006). Infrared Spectroscopy of Solid Hydrogen Sulfide and Deuterium Sulfide. *J. Phys. Chem. A* **110**, 10793. doi: 10.1021/jp0634104
- Frank, L.A., Paterson, W.R. (1999). Intense Electron Beams Observed at Io with the Galileo Spacecraft. *J. Geophys. Res. Space Phys.* **104**, 28657. doi: 10.1029/1999JA900402
- Furuya, K., Oba, Y., Shimonishi, T. (2022). Quantifying the Chemical Desorption of H₂S and PH₃ from Amorphous Water-Ice Surfaces. *Astrophys. J.* **926**, 171. doi: 10.3847/1538-4357/ac4260
- Garozzo, M., Fulvio, D., Gomis, O., Palumbo, M.E., Strazzulla, G. (2008). H-Implantation in SO₂ and CO₂ Ices. *Planet. Space Sci.* **56**, 1300. doi:10.1016/j.pss.2008.05.002
- Gomis, O., Strazzulla, G. (2008). Ion Irradiation of H₂O Ice on Top of Sulphurous Solid Residue and its Relevance to the Galilean Satellites. *Icarus* **194**, 146. doi: 10.1016/j.icarus.2007.09.015
- Guldan, E.D., Schindler, L.R., Roberts, J.T. (1995). Growth and Characterisation of Sulphuric Acid under Ultrahigh Vacuum. *J. Phys. Chem.* **99**, 16059. doi: unknown
- Herczku, P., Mifsud, D.V., Ioppolo, S., Juhász, Z., Kaňuchová, Z., Kovács, S.T.S., Traspas Muiña, A., Hailey, P.A., Rajta, I., Vajda, I., Mason, N.J., McCullough, R.W., Paripás, B., Sulik, B. (2021). The Ice Chamber for Astrophysics-Astrochemistry (ICA): A New Experimental Facility for Ion Impact Studies of Astrophysical Ice Analogues. *Rev. Sci. Instrum.* **92**, 084501. doi: 10.1063/5.0050930
- Hudson, R.L., Moore, M.H., Dworkin, J.P., Martin, M.P., Pozun, Z.D. (2008). Amino Acids from Ion-Irradiated Nitrile-Containing Ices. *Astrobiology* **8**, 771. doi: 10.1089/ast.2007.0131
- Hudson, R.L., Gerakines, P.A. (2018). Infrared Spectra and Interstellar Sulfur: New Laboratory Results for H₂S and Four Malodorous Thiol Ices. *Astrophys. J.* **867**, 138. doi: 10.3847/1538-4357/aac52a

- Ivlev, A.V., Giuliano, B.M., Juhász, Z., Herczku, P., Sulik, B., Mifsud, D.V., Kovács, S.T.S., Rahul, K.K., Rác, R., Biri, S., Rajta, I., Vajda, I., Mason, N.J., Ioppolo, S., Caselli, P. (2022). Radiolysis and Sputtering of CO Ice by Cosmic Rays: I. Experimental Insights into the Underlying Mechanisms. *Astrophys. J.* submitted
- Jiménez-Escobar, A., Muñoz-Caro, G.M. (2011). Sulfur Depletion in Dense Clouds and Circumstellar Regions. I. H₂S Ice Abundance and UV-Photochemical Reactions in the H₂O Matrix. *Astron. Astrophys.* **536**, 91. doi: 10.1051/0004-6361/201014821
- Jiménez-Escobar, A., Muñoz-Caro, G.M., Chen, Y.-J. (2014). Sulfur Depletion in Dense Clouds and Circumstellar Regions. Organic Products Made from UV Photoprocessing of Realistic Ice Analogues Containing H₂S. *Mon. Not. R. Astron. Soc.* **443**, 343. doi: 10.1093/mnras/stu1100
- Kitajima, K., Nakai, Y., Sameera, W.M.C., Tsuge, M., Miyazaki, A., Hidaka, H., Kouchi, A., Watanabe, N. (2021). Delivery of Electrons by Proton-Hole Transfer in Ice at 10 K: Role of Surface OH Radicals. *J. Phys. Chem. Lett.* **12**, 704. doi: 10.1021/acs.jpcclett.0c03345
- Kleeberg, H., Luck, W.A.P. (1989). Experimental Tests of the H-Bond Cooperativity. *Z. Phys. Chemie.* **270**, 613. doi: 10.1515/zpch-1989-27072
- Kouchi, A., Kuroda, T. (1990). Amorphisation of Cubic Ice by Ultraviolet Irradiation. *Nature* **344**, 134. doi: 10.1038/344134a0
- Laas, J.C., Caselli, P. (2019). Modelling Sulphur Depletion in Interstellar Clouds. *Astron. Astrophys.* **624**, A108. doi: 10.1051/0004-6361/201834446
- Mason, N.J., Nair, B., Jheeta, S., Szymańska, E. (2014). Electron Induced Chemistry: A New Frontier in Astrochemistry. *Faraday Discuss.* **168**, 235. doi: 10.1039/C4FD00004H
- Mason, N.J., Hailey, P.A., Mifsud, D.V., Urquhart, J.S. (2021). Systems Astrochemistry: A New Doctrine for Experimental Studies. *Front. Astron. Space Sci.* **8**, 739046. doi: 10.3389/fspas.2021.739046
- McGuire, B.A., Burkhardt, A.M., Loomis, R.A., Shingledecker, C.N., Lee, K.L.K., Charnley, S.B., Cordiner, M.A., Herbst, E., Kalenskii, S., Momjian, E., Willis, E.R., Xue, C., Remijan, A.J., McCarthy, M.C. (2020). Early Science from GOTHAM: Project Overview, Methods, and the Detection of Interstellar Propargyl Cyanide (HCCCH₂CN) in TMC-1. *Astrophys. J. Lett.* **900**, L10. doi: 10.3847/2041-8213/aba632
- Mifsud, D.V., Kaňuchová, Z., Herczku, P., Ioppolo, S., Juhász, Z., Kovács, S.T.S., Mason, N.J., McCullough, R.W., Sulik, B. (2021a). Sulfur Ice Astrochemistry: A Review of Laboratory Studies. *Space Sci. Rev.* **217**, 14. doi: 10.1007/s11214-021-00792-0
- Mifsud, D.V., Juhász, Z., Herczku, P., Kovács, S.T.S., Ioppolo, S., Kaňuchová, Z., Czentye, M., Hailey, P.A., Traspas Muiña, A., Mason, N.J., McCullough, R.W., Paripás, B., Sulik, B. (2021b). Electron Irradiation and Thermal Chemistry Studies of Interstellar and Planetary Ice Analogues at the ICA Astrochemistry Facility. *Eur. Phys. J. D: Atom. Mol. Opt. Plasma Phys.* **75**, 182. doi: 10.1140/epjd/s10053-021-00192-7
- Mifsud, D.V., Kaňuchová, Z., Ioppolo, S., Herczku, P., Traspas Muiña, A., Field, T.A., Hailey, P.A., Juhász, Z., Kovács, S.T.S., Mason, N.J., McCullough, R.W., Pavithraa, S., Rahul, K.K., Paripás, B., Sulik, B., Chou, S.-L., Lo, J.-I., Das, A., Cheng, B.-M., Rajasekhar, B.N., Bhardwaj, A., Sivaraman, B. (2022a). Mid-IR and VUV Spectroscopic Characterization of Thermally Processed and Electron Irradiated CO₂ Astrophysical Ice Analogues. *J. Mol. Spectrosc.* **385**, 111599. doi: 10.1016/j.jms.2022.111599
- Mifsud, D.V., Hailey, P.A., Herczku, P., Sulik, B., Juhász, Z., Kovács, S.T.S., Kaňuchová, Z., Ioppolo, S., McCullough, R.W., Paripás, B., Mason, N.J. (2022b). Comparative Electron Irradiations of Amorphous and Crystalline Astrophysical Ice Analogues. *Phys. Chem. Chem. Phys.* **24**, 10974. doi: 10.1039/d2cp00886f
- Mifsud, D.V., Hailey, P.A., Herczku, P., Juhász, Z., Kovács, S.T.S., Sulik, B., Ioppolo, S., Kaňuchová, Z., McCullough, R.W., Paripás, B., Mason, N.J. (2022c). Laboratory Experiments on the Radiation Astrochemistry of Water Ice Phases. *Eur. Phys. J. D: Atom. Mol. Opt. Plasma Phys.* **76**, 87. doi: 10.1140/epjd/s10053-022-00416-4

- Moore, M.H., Ferrante, R.F., Hudson, R.L., Stone, J.N. (2007a). Ammonia-Water Ice Laboratory Studies Relevant to Outer Solar System Surfaces. *Icarus* **190**, 260. doi: 10.1016/j.icarus.2007.02.020
- Moore, M.H., Hudson, R.L., Carlson, R.W. (2007b). The Radiolysis of SO₂ and H₂S in Water Ice: Implications for the Icy Jovian Satellites. *Icarus* **189**, 409. doi: 10.1016/j.icarus.2007.01.018
- Muñoz Caro, G.M., Meierhenrich, U.J., Schutte, W.A., Barbier, B., Arcones Segovia, A., Rosenbauer, H., Thiemann, W.H.-P., Brack, A., Greenberg, J.M. (2002). Amino Acid from Ultraviolet Irradiation of Interstellar Ice Analogues. *Nature* **416**, 403. doi: 10.1038/416403a
- Navarro-Almaida, D., Le Gal, R., Fuente, A., Rivière-Marichalar, P., Wakelam, V., Cazaux, S., Caselli, P., Laas, J.C., Alonso-Albi, T., Loison, J.C., Gerin, M., Kramer, C., Roueff, E., Bachiller, R., Commerçon, B., Friesen, R., García-Burillo, S., Goicoechea, J.R., Giuliano, B.M., Jiménez-Serra, I., Kirk, J.M., Lattanzi, V., Malinen, J., Marcelino, N., Martín-Domènech, R., Muñoz-Caro, G.M., Pineda, J., Tercero, B., Treviño-Morales, S.P., Roncero, O., Hacar, A., Tafalla, M., Ward-Thompson, D. (2020). Gas Phase Elemental Abundances in Molecular CloudS (GEMS) II. On the Quest for the Sulphur Reservoir in Molecular Clouds: The H₂S Case. *Astron. Astrophys.* **637**, A39. doi: 10.1051/0004-6361/201937180
- Noll, K.S., Johnson, R.E., McGrath, M.A., Caldwell, J.J. (1997). Detection of SO₂ on Callisto with the Hubble Space Telescope. *Geophys. Res. Lett.* **24**, 1139. doi: 10.1029/97GL00876
- Noll, K.S., Weaver, H.A., Gonnella, A.M. (1998). The Albedo Spectrum of Europa from 2200 Å to 3300 Å. *J. Geophys. Res. Planet.* **100**, 19057. doi: 10.1029/94JE03294
- Nuevo, M., Milam, S.N., Sandford, S.A. (2012). Nucleobases and Prebiotic Molecules in Organic Residues Produced from the Ultraviolet Photo-Irradiation of Pyrimidine in NH₃ and H₂O+NH₃ Ices. *Astrobiology* **12**, 295. doi: 10.1089/ast.2011.0726
- Oba, Y., Tomaru, T., Lamberts, T., Kouchi, A., Watanabe, N. (2018). An Infrared Measurement of Chemical Desorption from Interstellar Ice Analogues. *Nature Astron.* **2**, 228-232. doi: 10.1038/s41550-018-0380-9
- Oba, Y., Tomaru, T., Kouchi, A., Watanabe, N. (2019). Physic-Chemical Behaviour of Hydrogen Sulphide Induced by Reactions with H and D Atoms on Different Types of Ice Surfaces at Low Temperature. *Astrophys. J.* **874**, 124. doi: 10.3847/1538-4357/ab0961
- Pellegrini, A., Ferro, D.R., Zerbi, G. (1973). Dynamics and Structure of Disordered Hydrogen-Bonded Crystals: Methanol. *Mol. Phys.* **26**, 577. doi: 10.1080/00268977300101911
- Pilling, S., Bergantini, A. (2015). The Effect of Broadband and Soft X-Rays in SO₂-Containing Ices: Implications on the Photochemistry of Ices Toward Young Stellar Objects. *Astrophys. J.* **811**, 151. doi: 10.1088/0004-637X/811/2/151
- Post, B., Schwartz, R.S., Fankuchen, I. (1952). The Crystal Structure of Sulphur Dioxide. *Acta Crystall.* **5**, 372. doi: 10.1107/s0365110x5200109x
- Rubin, M., Engrand, C., Snodgrass, C., Weissman, P., Altwegg, K., Busemann, H., Morbidelli, A., Mumma, M. (2020). On the Origin and Evolution of the Material in 67P/Churyumov-Gerasimenko. *Space Sci. Rev.* **216**, 102. doi: 10.1007/s11214-020-00718-2
- Ruffle, D.P., Hartquist, T.W., Caselli, P., Williams, D.A. (1999). The Sulphur Depletion Problem. *Mon. Not. R. Astron. Soc.* **306**, 691. doi: 10.1046/j.1365-8711.1999.02562.x
- Schriver-Mazzuoli, L., Chaabouni, H., Schriver, A. (2003). Infrared Spectra of SO₂ and SO₂:H₂O at Low Temperature. *J. Mol. Struct.* **644**, 151. doi: 10.1016/S0022-2860(02)00477-5
- Shingledecker, C.N., Lamberts, T., Laas, J.C., Vasyunin, A., Herbst, E., Kästner, J., Caselli, P. (2020). Efficient Production of S₈ in Interstellar Ices: The Effects of Cosmic-Ray-Driven Radiation Chemistry and Nondiffusive Bulk Reactions. *Astrophys. J.* **888**, 52. doi: 10.3847/1538-4357/ab5360

- Sivaraman, B., Jamieson, C.S., Mason, N.J., Kaiser, R.I. (2007). Temperature-Dependent Formation of Ozone in Solid Oxygen by 5 keV Electron Irradiation and Implications for Solar System Ices. *Astrophys. J.* **669**, 1414. doi: 10.1086/521216
- Sum, A.K., Sandler, S.I. (2000). *Ab Initio* Calculations of Cooperativity Effects on Clusters of Methanol, Ethanol, 1-Propanol, and Methanethiol. *J. Phys. Chem. A* **104**, 1121. doi: 10.1023/jp993094b
- Tieftrunk, A., Pineau des Forêts, G., Shilke, P., Walmsley, C.M. (1994). SO and H₂S in Low Density Molecular Clouds. *Astron. Astrophys.* **289**, 579. doi: unknown
- Vidal, T.H.G., Loison, J.-C., Jaziri, A.Y., Ruaud, M., Gratier, P., Wakelam, V. (2017). On the Reservoir of Sulphur in Dark Clouds: Chemistry and Elemental Abundance Reconciled. *Mon. Not. R. Astron. Soc.* **469**, 435. doi: 10.1093/mnras/stx828
- Wallner, M., Jarraya, M., Olsson, E., Ideböhn, V., Squibb, R.J., Ben Yaghlane, S., Nyman, G., Eland, J.H.D., Feifel, R., Hochlaf, M. (2022). Abiotic Molecular Oxygen Production – Ionic Pathway from Sulphur Dioxide. *Science Adv.* **8**, eabq5411. doi: 10.1126/sciadv.abq5411
- Yarnall, Y.Y., Hudson, R.L. (2022). Crystalline Ices – Densities and Comparisons for Planetary and Interstellar Applications. *Icarus* **373**, 114799. doi: 10.1016/j.icarus.2021.114799